

REPORT DOCUMENTATION PAGE*Form Approved
OMB No. 0704-0188*

The public reporting burden for this collection of information is estimated to average 1 hour per response, including the time for reviewing instructions, searching existing data sources, gathering and maintaining the data needed, and completing and reviewing the collection of information. Send comments regarding this burden estimate or any other aspect of this collection of information, including suggestions for reducing the burden, to the Department of Defense, Executive Services and Communications Directorate (0704-0188). Respondents should be aware that notwithstanding any other provision of law, no person shall be subject to any penalty for failing to comply with a collection of information if it does not display a currently valid OMB control number.

PLEASE DO NOT RETURN YOUR FORM TO THE ABOVE ORGANIZATION.

1. REPORT DATE (DD-MM-YYYY)		2. REPORT TYPE		3. DATES COVERED (From - To)	
4. TITLE AND SUBTITLE				5a. CONTRACT NUMBER	
				5b. GRANT NUMBER	
				5c. PROGRAM ELEMENT NUMBER	
6. AUTHOR(S)				5d. PROJECT NUMBER	
				5e. TASK NUMBER	
				5f. WORK UNIT NUMBER	
7. PERFORMING ORGANIZATION NAME(S) AND ADDRESS(ES)				8. PERFORMING ORGANIZATION REPORT NUMBER	
9. SPONSORING/MONITORING AGENCY NAME(S) AND ADDRESS(ES)				10. SPONSOR/MONITOR'S ACRONYM(S)	
				11. SPONSOR/MONITOR'S REPORT NUMBER(S)	
12. DISTRIBUTION/AVAILABILITY STATEMENT					
13. SUPPLEMENTARY NOTES					
14. ABSTRACT					
15. SUBJECT TERMS					
16. SECURITY CLASSIFICATION OF:			17. LIMITATION OF ABSTRACT	18. NUMBER OF PAGES	19a. NAME OF RESPONSIBLE PERSON
a. REPORT	b. ABSTRACT	c. THIS PAGE			19b. TELEPHONE NUMBER (Include area code)

PUBLICATION OR PRESENTATION RELEASE REQUEST

15-1231-1320

Pubkey 3676

NRLINST 5510 40

1. REFERENCES AND ENCLOSURES		2. TYPE OF PUBLICATION OR PRESENTATION		3. ADMINISTRATIVE INFORMATION			
Ref: (a) NRL Instruction 5800.2 (b) NRL Instruction 5510.40E Encl: (1) Two copies of subject publication/presentation		<input type="checkbox"/> Abstract only, published <input type="checkbox"/> Book author <input type="checkbox"/> Book editor <input checked="" type="checkbox"/> Conference Proceedings (referred) <input type="checkbox"/> Journal article (referred) <input type="checkbox"/> Oral Presentation, published <input type="checkbox"/> Video <input type="checkbox"/> Poster ALL DOCUMENTS/PRESENTATIONS MUST BE ATTACHE		<input type="checkbox"/> Abstract only, not published <input type="checkbox"/> Book chapter <input type="checkbox"/> Multimedia report <input type="checkbox"/> Conference Proceedings (not referred) <input type="checkbox"/> Journal article (not referred) <input type="checkbox"/> Oral Presentation, not published <input type="checkbox"/> Other, explain		STRN NRL/PP/7330-15-2535 Route Sheet No. 7330/ Job Order No. 73-1951-05-5 Classification U S C FOUO Sponsor ONR BASE <i>6/1 Bay</i> Sponsor's approval <input type="checkbox"/> yes* (attached) (*Required if research is otheran E 1/B 2 NRL or ONR unclassified research or publication/presentation is classified)	

4. AUTHOR

Title of Paper or Presentation
 Fiber-optic anemometer based on silicon Fabry-Perot interferometer

AUTHOR(S) LEGAL NAMES(S) OF RECORD (First, MI, Last), CODE, (Affiliation if not NRL).
 Guigen Liu University of Nebraska-Lincoln, Weilin Hou 7333, Ming Han University of Nebraska-Lincoln,

This paper will be presented at the OSA Imaging and Applied Optics Meeting
 (Name of Conference)

07-JUN - 11-JUN-15, Arlington, VA, Unclassified
 (Date, Place and Classification of Conference)

and/or for published in OSA Imaging and Applied Optics Meeting, Unclassified
 (Name and Classification of Publication) (Name of Publisher)

5. CERTIFICATION OR CLASSIFICATION

It is my opinion that the subject paper (is) (is not) classified, in accordance with reference (b) and this paper does not violate any disclosure of trade secrets or suggestions of outside individuals or concerns which have been communicated to the NRL in confidence.

This subject paper (has) (has never) been incorporated in an official NRL Report.

Weilin Hou, 7333 *[Signature]*
 Name and Code (Principal Author) (Legal Name of Record and Signature Only) (Signature)

6. ROUTING-APPROVAL (NOTE: If name other than your legal name of record is annotated on the publication or presentation itself, add an explanatory note in the "Comments" section below next to your signed legal name of record)

CODE	SIGNATURE	DATE	COMMENTS
Co-Author(s) Weilin Hou, 7333	<i>[Signature]</i>	4/8/15	Need by 29 Apr 2015
Section Head	<i>[Signature]</i>		This is a Final Security Review. Any changes made in the document, after approved by Code 1231, nullify the Security Review.
Branch Head Richard L. Groat, 7330	<i>[Signature]</i>	4-8-2015	
Division Head Ruth H. Preller, 7300	<i>[Signature]</i>	4/9/15	1. To the best knowledge of this Division, the subject matter of this publication (has <input type="checkbox"/>) (has never <input checked="" type="checkbox"/>) been classified. 2. This paper (does <input type="checkbox"/>) (does not <input checked="" type="checkbox"/>) contain any militarily critical technology.
ADOR/Director NCST E. R. Franch, 7000			
SECURITY			
Security, Code 1231	<i>[Signature]</i>	4/20/15	A copy of the paper, abstract or presentation is filed in this office.
Associate Counsel Code 1008 3	<i>[Signature]</i>	5/7/2015	
Public Affairs (Unclassified/Unlimited Only), Code 7030 4	<i>[Signature]</i>	4-27-15	
Division, Code			
Author, Code			

15 APR 15 10:22

Fiber-optic anemometer based on silicon Fabry-Pérot interferometer

Guigen Liu¹, Weilin Hou², Wei Qiao¹, and Ming Han^{1,*}

¹Department of Electrical Engineering, University of Nebraska-Lincoln, Lincoln, NE 68588, USA

²Naval Research Laboratory, Code 7333, Stennis Space Center, MS 39529, USA

* Corresponding author: mhan3@unl.edu

ABSTRACT

Flowmeters have been finding vast applications in all kinds of industrial processes, such as process control, food quality surveillance, wind turbines, environment monitoring, etc. In this paper, we propose a new anemometer which consists of a Fabry-Pérot interferometer (FPI) implemented using a thin silicon mounted on the tip of an optical fiber. The anemometer takes advantage of the superior thermal and optical properties of silicon. Silicon is transparent to infrared wavelength, while it absorbs visible light. Thus, the silicon FPI can be heated by a beam injected from a red diode laser while the infrared signals go through it without any interference from the heating light. The heat loss from the silicon film will increase when the sensor is placed in stronger flow (wind), which induces a decrease in the optical path of the silicon FPI, which lead to blueshifts the output spectrum. A higher wind speed corresponds to a larger wavelength shift. By tuning the heating power, the response range and sensitivity of the anemometer is changed. Experimental results demonstrate that a wavelength shift -0.574 nm was observed for a wind speed of 4 m/s. Better sensitivity is to be expected when stronger heating applied. The proposed sensor also features simple structure, low cost and fast response.

Keywords: Fiber-optic sensors, anemometer, Fabry-Pérot interferometer, silicon film, thermal effects.

1. INTRODUCTION

Over the last decade, fiber-optic sensors based on hot-wire scheme have attracted a great deal of attention [1-5], due to the advantages of active sensors, such as controllable sensitivity that can be adapted to a changing environment, over the passive ones. These fiber-optic hot-wire anemometers are based on a laser-heated fiber Bragg grating (FBG), which proves a promising alternative to conventional hot-wire anemometers based on thermocouples [6], due to the inherent advantages such as immunity to strong external electromagnetic interference, resistance to hostile environment, simple configuration and low cost, just to name a few. For these hot-wire based FBG anemometers, a heating laser light source is exerted either externally [2] or internally [1, 3-5] to introduce a temperature difference between the FBG and surroundings. The sensors become active when there is a controllable heating source, which is a big advantage for easy adjustments when the sensors are mounted in a varying environment. When the incoming winds blow against the sensor, the cooling affects blueshift the resonance wavelength of the FBG. The higher the wind speed, the larger the wavelength blueshift. Consequently, the wind speed is inferred from the amount of the blueshift of the Bragg wavelength. It is obvious that the external heating scheme makes the system bulky and inflexible, which is limited when highly-integrated system is required. Instead, a more convenient way to heat the FBG can be realized internally by transmitting the heating laser light within the same fiber. In the internal heating method, either an absorbing coating is applied on the outer surface of the FBG [1, 4] or a highly-absorbing fiber is used to convert the heating laser to the promoted temperature of the sensor [3, 5]. Obviously, an extra metal (gold or silver) coating or an extra high absorption fiber would make the fabrication process more complicated and costly. Furthermore, the length of FBG (usually several millimeters long) makes it infeasible when it comes to high spatial resolution. Therefore, it would definitely extend the applications of a fiber-optic anemometer if the advantages of hot-wire configuration is conserved while the limitations on the existing forms are avoided.

We have presented a novel miniature fiber-optic anemometer based on hot-wire scheme [7]. It is composed of a thin silicon disk that is glued on the tip of a single-mode fiber (SMF) and works as a Fabry-Pérot interferometer (FPI). Dip wavelength in the reflection spectrum is sensitively dependent on temperature of silicon FPI. Since silicon is highly absorptive in visible wavelength while highly transparent in infrared range, a red laser diode is applied as a heating source while a broadband infrared light source serves as the probing signal. Like other FBG hot-wire anemometers, the reflection wavelength is blueshifted in response to the cooling effects brought about by the air flow. Since no extra coating or other structure is needed, the sensor under investigation is simple, low-cost and flexible for operation, while preserving the other advantages of hot-wire anemometry. Furthermore, the miniature footprint, i.e. the thin silicon disk, has a diameter less than that of silica fiber cladding (125 μm) and a thickness of only 10 μm . This endows the sensor

with great promise for applications where high spatial resolution or limited mounting space is required. In this paper, more details are provided on the sensor proposed in [7], including the sensor fabrication, sensor response to laser heating, and repeatability in response to the fast varying wind speed in the turbulent air flow.

2. OPERATION PRINCIPLE

Schematic representation of the specific sensor head is shown in Fig. 1(a) [7]. A piece of thin silicon disk is fixed on the tip of a piece of SMF. The silicon disk is heated by a laser diode. The operation principle of this sensor is briefly illustrated in Fig. 1(b). The silicon disk works as a thin FPI which involves two reflections from the fiber-silicon and silicon-surrounding interfaces. Reflection spectrum of the silicon FPI features fringe dips which are dependent on temperature through thermo-optic and thermal expansion effects. Consequently, variation of the temperature of the silicon disk is measured through monitoring shift in the dip wavelength. Due to the high transparency of silicon in infrared wavelength, a broadband source centered around 1550 nm is used to serve as the signal light. High opacity of silicon in the visible range makes a red laser diode a perfect heating light source. When the silicon disk is heated by laser, the dip wavelength is redshifted from the original position due to elevated silicon temperature, as shown by the blue and solid red curves in Fig. 1(c). When wind blows over its surface, heat losses occur due to the temperature gradient between silicon and air. This cooling effect is balanced between heating with a fixed power and chilling by the wind with a constant speed, leading to a resulting blueshift of the dip wavelength, as illustrated by the dashed and solid red curves in Fig. 1(c). The higher the wind speed, the more significant the blueshift. Therefore, the wind speed can be derived by examining the amount of blueshift.

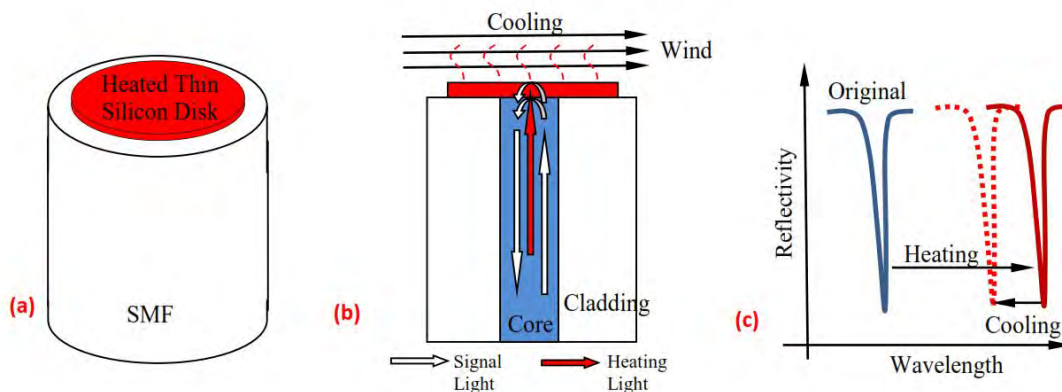


Figure 1. Sketch of the (a) sensor configuration and (b) operation principle. (c) Redshift of the dip wavelength in response to heating by laser and blueshift in response to cooling by wind.

3. EXPERIMENTS

3.1 System

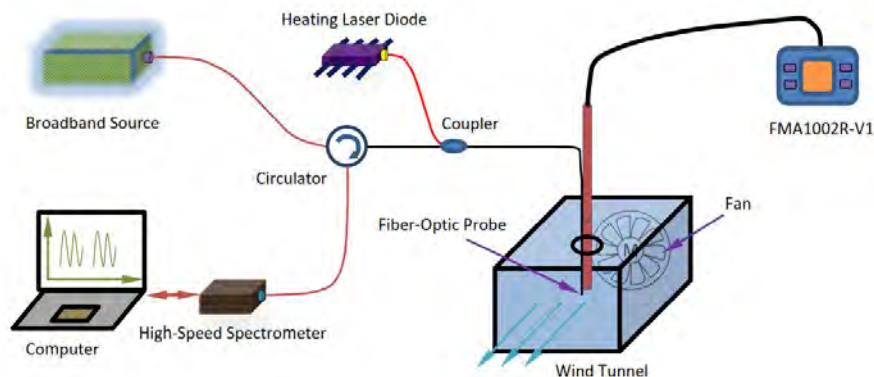


Figure 2. Schematic of the experimental arrangement.

The experimental setup is described in Ref. [7] and shown in Fig. 2. A high-power broadband source (AFOL-ASE-C13, Acronym Fiber Optics, Inc.) provided the signal light source to the sensor probe via a circulator. Laser diode (LPS-635-FC, Thorlabs) emitted at wavelength of 635 nm as the heating light to the silicon disk via a coupler. The reflected spectrum was collected by a high-speed spectrometer (I-MON 256, Ibsen Photonics). A laptop computer is used to control the sampling rate and integral time of the spectrometer, and to record the data. The fiber probe was attached to a commercial thermocouple hot-wire anemometer (FMA1002R-V1, OMEGA), which served as both calibration and reference. The sensors were placed in a crude wind tunnel driven by a motorized fan with controllable speed.

3.2 Sensor Fabrication

To fabricate the sensor, the thin silicon disks were first fabricated through micro-electro-mechanical system (MEMS) fabrication technology. Briefly, a 10- μm -thick double-side-polished thin silicon wafer, which was purchased from Virginia Semiconductor, was patterned into small disks with a diameter of 100 μm using photoresist; then, the chemicals attacked the etching grooves with a depth of 8 μm , leaving a thickness of around 2 μm to prevent the bottom side of the disk from being etched, and to assist disposition of the silicon disk during washing of the residual photoresist. Lastly, the cleaned and dry patterned silicon wafer was broken into separate small round disks by careful manipulation under a microscope.

With the small disks ready, the process to mount a silicon disk on the cleaved tip of a SMF is schematically shown in Fig. 3. Firstly, a silicon disk was placed on another large clean silicon wafer working as a substrate, as shown in Fig. 3(a). Secondly, a thin film of UV curable glue was formed on a piece of glass slide by spinning coating, then the glue film was transferred to the cleaved endface of a section of stripped and cleaned SMF by vertically dipping the fiber tip toward the glue film and then lifting it up under an optical microscope. This step is illustrated in Fig. 3(b). Thirdly, the fiber tip with glue film was adjusted and pressed on the thin silicon disk, followed by a UV light irradiation for around 5 min, which is depicted in Fig. 3(c). After the glue was cured, a mounted sensor shown in Fig. 3(d) was obtained. Similar fabrication steps were applied in our previous work on the high-resolution and high-speed temperature sensor [8].

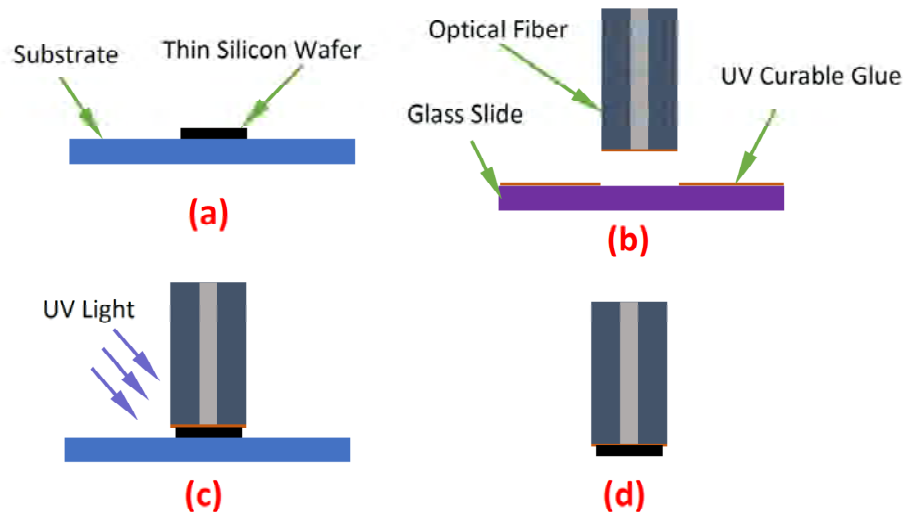


Figure 3. Brief illustration of the fabrication steps of the fiber-optic probe. (a) Patterning the thin silicon wafer into small pieces. (b) Applying UV curable glue on the end of a cleaved optical fiber. (c) Curing the glue by UV light. (d) Separating the sensor probe from the substrate.

3.3 Measurement of wind

Using the experimental setup shown in Fig. 2 and the fabricated sensors described in Section 3.2, response of the investigated sensor has been characterized. First, response of the reflection dip wavelength to the laser heating in the absence of wind is shown in Fig. 4(a). Obviously, heating by the laser promotes the silicon temperature and thus produces a redshift of the reflection dip wavelength. The higher the heat laser power (represented by the laser current), the larger the wavelength shift. The cooling effects brought by wind was examined and the result is shown in Fig. 4(a). When there is a wind blowing over the sensor head, some of thermal energy is lost by the cooling effect, leading to a

reduced silicon temperature, which is demonstrated in Fig. 4(b). The dip wavelength was stable when there was no wind present. It went down sharply, and showed large fluctuations when the wind was turned on. Large variation in the wavelength is believed to be due to the fast mixing process within the turbulent microstructure from the wind blowing over the top surface of the silicon disk [9]. The wind lasted for about 20 s and then was turned off. As the residual wind slowed down, the wavelength went up slowly again to the initial value before the wind was turned on, suggesting an excellent repeatability of the sensor.

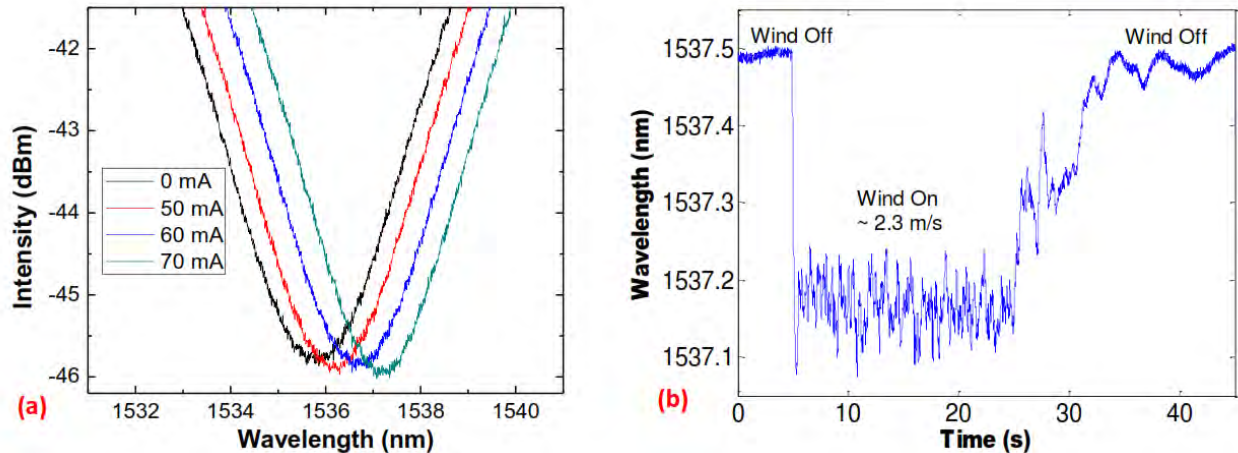


Figure 4. (a) Dip wavelength at different heating laser currents in the absence of wind. (b) Wavelength response of the sensor when wind was suddenly turned on for ~20 s and then off.

Next, the response of the fiber sensor to wind speed at different heating laser currents was measured and the results are shown in Fig. 5(a). Due to the large variation of wavelength which was caused by the turbulent local wind speeds, as shown in Fig. 4(b) when the wind was turned on, the average value of the fluctuating wavelength was calculated as the wavelength at this certain wind speed, while the standard deviation value as the error bar in Fig. 5(a). When there was no heating laser, the stable wavelength makes the error bar invisible (black square curve). Note that the wavelength went up as the wind speed increased, which is likely due to the slightly increased temperature of the surrounding air, as a function of the heat dissipation from the running motor of the fan driving the wind tunnel. Regardless of the slightly elevated wind temperature, the relative wavelength blueshifted as wind speed increased. It can also be seen that the larger the heating laser current, the more sensitive the sensor is. With a laser current of 70 mA, a wavelength shift of -0.574 nm was observed at the wind speed of 4 m/s. If the heating power is increased or the coupling efficiency of heating laser is increased, a higher sensitivity is expected.

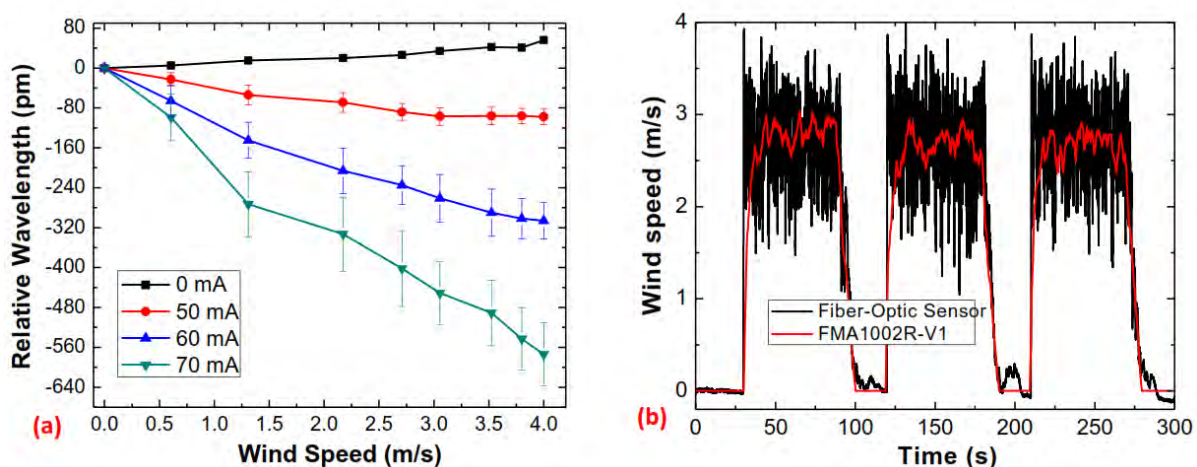


Figure 5. (a) Relative wavelength shift as a function of wind speed at different heating laser currents. (b) Response comparison between the fiber sensor and commercial anemometer. Note that wind speeds of the fiber-optic anemometer were calibrated by the commercial FMA1002R-V1 anemometer.

In addition to the controllable sensitivity, the proposed sensor is also fast in response with excellent repeatability. Fig. 5(b) shows the comparison between the fiber sensor and the commercial sensor in response to three cycles of turning on and off the wind tunnel. It is apparent that in addition to the visualization of large variation of local wind speed, the steeper rising of the fiber sensor output than that of the commercial sensor well suggested the fast response (much less than 1 second) of the fiber anemometer. Also, the sensor outputted the same level for the three times when the wind was turned on, and the output went back to zero when wind was turned off, suggesting the reliable repeatability.

4. CONCLUSION

We have demonstrated a novel fiber-optic anemometer, implemented by attaching a thin silicon disk on the cleaved tip of a SMF. The silicon disk works as a FPI from which the dip wavelength in the reflection spectrum is monitored, which is dependent on the silicon temperature. By applying a heating laser, temperature of the silicon is promoted above the surroundings. When air flows over the sensor head, cooling effects reduce the silicon temperature which leads to blueshifts of the dip wavelength. A higher rate of air flow produces a more pronounced blueshift. In experiments, a wavelength shift of -0.574 nm was obtained for the wind speed of 4 m/s. The sensitivity can be easily controlled by adjusting the heat laser power. This novel sensor also features fast response, with a rising time significantly less than 1 second.

5. ACKNOWLEDGEMENT

This work was partially supported U.S. Naval Research Laboratory under contract no. N0017315P0376 and U.S. Office of Naval Research under grant no. N000141310159. The authors thank Dr. Jiong Hua at NCMN of UNL for helping fabricate the silicon disks. Stimulating discussions with Prof. Zhaoyan Zhang on the heat-transfer problem and technical supports from Mr. Dustin Dam on the high-speed spectrometer are highly appreciated.

6. REFERENCE

- [1] K. P. Chen, B. McMillen, M. Buric, and C. Jewart, "Self-heated fiber Bragg grating sensors," *Appl. Phys. Lett.* **86**, 143502 (2005).
- [2] D. W. Lamb, and A. Hooper, "Laser-optical fiber Bragg grating anemometer for measuring gas flows: application to measuring the electric wind," *Opt. Lett.* **31**, 1035-1037 (2006).
- [3] S. Gao, A. P. Zhang, H.-Y. Tam, L. H. Cho, and C. Lu, "All-optical fiber anemometer based on laser heated fiber Bragg gratings," *Opt. Express* **19**, 10124-10130 (2011).
- [4] X. Wang, X. Dong, Y. Zhou, K. Ni, J. Cheng, and Z. Chen, "Hot-wire anemometer based on silver-coated fiber Bragg grating assisted by no-core fiber," *IEEE Photon. Technol. Lett.* **25**, 2458-2461 (2013).
- [5] R. Chen, A. Yan, Q. Wang, and K. P. Chen, "Fiber-optic flow sensors for high-temperature environment operation up to 800 °C," *Opt. Lett.* **39**, 3966-3969 (2014).
- [6] S. Takagi, "A hot-wire anemometer compensated for ambient temperature variations," *J. Phys. E: Sci. Instrum.* **19**, 739-743 (1986).
- [7] G. Liu, W. Hou, W. Qiao, and M. Han, "A fast-reponse fiber-optic anemometer with temperature self-compensation", submitted.
- [8] G. Liu, M. Han, and W. Hou, "High-resolution and fast-response fiber-optic temperature sensor using silicon Fabry-Pérot cavity " *Opt. Express* **23**, 7237-7247 (2015).
- [9] M. N. Özışık, *Heat transfer: a basic approach* (McGraw-Hill, Inc, New York, 1985).